2019

Formation of Low-Density and Free-Flowing Hollow Microparticles from Butter and Fractionated Palm Oil Mixture

Joshua Gudeman
University of Nebraska-Lincoln, josh.gudeman@gmail.com

Junsi Yang
University of Nebraska-Lincoln, junsiyang@huskers.unl.edu

Ozan Ciftci
University of Nebraska-Lincoln, ciftci@unl.edu

Formation of Low-Density and Free-Flowing Hollow Microparticles from Butter and Fractionated Palm Oil Mixture

Joshua Gudeman, Junsi Yang, and Ozan N. Ciftci

Department of Food Science and Technology, University of Nebraska–Lincoln, 1901 N. 21 St. Food Innovation Center, Lincoln, NE 68588-6205, USA

Corresponding author — Ozan N. Ciftci, ciftci@unl.edu

Abstract

The use of solid fats is challenging due to difficulty in incorporating into foods, handling during industrial food production, and relatively high-calorie contributions. The objective of this study was to form free-flowing and low-density hollow microparticles from nonhydrogenated fats, namely, butter and fractionated palm oil, using a novel method based on atomization of a carbon dioxide (CO_2)- expanded lipid mixture. The melting point of the fractionated palm oil decreased from 66.2 to 47.3°C above 120 bar in the presence of pressurized CO_2. The density of the particles decreased five-folds compared to that of the original oils. The average particle size D [4,3] decreased from 67.0 to 27.1 μm when the concentration of fractionated palm oil was increased from 50% to 100%. The hollow structure was more pronounced for the particles obtained from higher melting oils/oil blends, as well as with more spherical uniformity. Ten percent ($d_{10\%}$) and 50% ($d_{50\%}$) of the palm oil particles were smaller than 4.5 and 23.0 μm, respectively, whereas they were 14.5 and 58.3 μm when mixed with butter at 50% butter concentration, respectively. Polymorphic form of α was more pronounced

Published in *Journal of the American Oil Chemistry Society* 96 (2019), pp 147–158.
doi 10.1002/aocs.12171

Submitted 12 March 2018; revised 24 September 201; accepted 25 September 2018; published 2 December 2018.

in the solid lipid particles, indicating that they had a less-ordered crystalline structure than the original oil. This new method forms low-density and free-flowing lipid powders that make the handling and storage of solid lipids feasible and convenient, and may provide reduced fat usage and calorie intake, and more rapid oil melting in mouth.

Keywords: Fractionated palm oil, Butter, Hollow solid lipid particle, Supercritical carbon dioxide, Melting

Introduction

Although solid fats are critical components of many foods, their use can present a number of challenges. In industrial food production, solid fats like butter and shortening can cause process inefficiencies. They are often packaged and stored in cubes or large totes that can be difficult to handle. Totes of solid fats require the use of heavy equipment to transport to ingredient-batching areas and usually need to be melted before incorporation into the batch. Cubes of solid fat are heavy and difficult for operators to add during batching. After being added to a batch mixture, many production procedures will then require a time-consuming waiting step to allow the solid oil to melt so it can be evenly dispersed throughout the ingredient mixture. Solid fats may also be stored in large bulk tanks at production plants, but bulk tank storage requires the oil to be heated above its melting point to be pumped. These elevated temperatures require costly energy to maintain and can also accelerate oil degradation. At a consumer level, cold butter can be difficult to spread evenly onto bread without the presence of butter clumps or potentially tearing the bread. When preparing baked goods like pastries, kneading butter and/or shortening into the dough can also be problematic. If the solid fat is not properly dispersed into the dough, the baked good will have an inconsistent and undesirable texture. A potential solution to these challenges is to create small solid fat particles that are free-flowing, easy-to-handle, and simple to be incorporated into foods.

The exciting role of supercritical fluid technology in particle formation has attracted interest in recent years (Fahim et al., 2014; Lubary et al., 2011; Ubeyitogullari and Ciftci, 2016; Yang and Ciftci, 2016). Carbon dioxide (CO_2) is the most common supercritical fluid because it has mild critical temperature and pressure (31°C, 74 bar), and it is nontoxic, nonflammable, environmentally friendly, inexpensive, and safe.

Previously, micron size solid lipid particles were generated using particle from gas-saturated solutions (PGSS) or gas-assisted melting atomization (GAMA) methods (Bertucco et al., 2007; García-González et al., 2010; Lubary et al., 2011; Mandžuka and Knez, 2008; Sampaio de Sousa et al., 2007). Lubary et al. (2011) used a similar process called supercritical melt micronization to form and collect the particles from nonchemically modified low-melting lipids, namely, anhydrous milk fat and a diacylglycerol-based modified milk fat. A potential challenge of that method was the development and maintenance of a low-temperature environment in the sample collection vessel, which could be resource intensive on an industrial scale. In addition, using low-melting lipids requires material handling at refrigerated temperatures after particle formation. Recently, Yang and Ciftci (2016) reported formation of hollow solid lipid microparticles and nanoparticles from fully hydrogenated soybean oil via atomization of a CO_2- expanded lipid through a nozzle. In the process of Yang and Ciftci (2016), upon depressurization, the Joule- Thomson effect caused cooling at the nozzle and the surrounding area, which allowed for crystallization of the liquid lipid bubble to form hollow solid lipid particles (Yang and Ciftci, 2016). To successfully produce solid lipid particles, the lipid material must have a melting point sufficiently above the ambient temperature where the CO_2- expanded lipid is being depressurized and atomized. Even though fully hydrogenated oils are suitable candidates for lipid particle formation using the method recently reported by Yang and Ciftci (2016) due to their high melting point, trans-free composition, and low cost, a potential issue with using hydrogenated oils is that many consumers have an aversion to seeing hydrogenated oils on a food's ingredient statement (Watson, 2018; Dietz and Scanlon, 2012; Downs et al., 2013). Nonhydrogenated oils and their blends are potential candidates to form such lipid particles but their behavior during particle formation via atomization of CO_2- expanded lipid is not known due to the wide melting range of nonhydrogenated oils resulting from the presence of a number of different triacylglycerols.

Therefore, the main objective of this study was to investigate the formation of free-flowing and low-density lipid microparticles composed of nonhydrogenated oils that can provide benefits such as easy handling, simple incorporation into foods, and improved food quality. Specific objectives were to: (i) form dry hollow solid lipid microparticles from fractionated palm oil and low-moisture butter using CO_2;

(ii) determine the melting behavior of fractionated palm oil and low-moisture butter in pressurized CO_2; and (iii) characterize the particles in terms of particle morphology, particle size and size distribution, particle density, melting properties, and polymorphism.

Materials and Methods

Materials

Fractionated palm oil was acquired from Loders Croklaan B.V. (Channahon, IL, USA). Low-moisture butter was acquired from Dairy Farmers of America Inc. (Kansas City, KS, USA). CO_2 (99.99% purity) was purchased from Matheson (Lincoln, NE, USA).

Preparation of the Fractionated Palm Oil and Butter Blends

Fractionated palm oil and low-moisture butter were separately melted on a hotplate at 130°C for 20 min to erase crystal memory. Then, oil blends were prepared by uniformly mixing fractionated palm oil and butter to obtain 25%, 50%, and 75% (v/v) butter contents in the blends.

Determination of Melting Behavior of the Solid Lipids in Pressurized Carbon Dioxide

Melting behavior of the fractionated palm oil and butter in pressurized CO_2 was studied in a jacketed high-pressure vessel according to Yang and Ciftci (2016). The high-pressure vessel was equipped with two sapphire windows, a microscope, a camera, and a refrigerated circulator (model 1162A, VWR Inc., Radnor, PA, USA). A circulating bath was used to control the temperature of the vessel by circulating hot and cold water through the jacket of the vessel. Each lipid sample was completely melted as previously described, and 100 µL of the molten lipid was placed into a 200 µL glass gas chromatograph (GC) vial

insert. Then, the GC vial insert was placed in a glass transparent vial and then positioned in the vessel chamber between the two sapphire windows. CO_2 was used to pressurize the vessel via a syringe pump (Model 250D, Teledyne Isco Inc., Lincoln, NE, USA). The molten lipid sample was stabilized in the pressurized chamber for 1 hour. Then, the temperature of the vessel was decreased to 5°C below the solidification temperature of the lipid, which was observed using the microscope-camera system. After 5 min of complete solidification, temperature of the vessel was increased at a rate of 0.3°C min^{-1} to observe the first melting point of each lipid sample. The first melting temperature and corresponding pressure were recorded.

Production of Hollow Solid Butter-Palm Oil Microparticles Using Carbon Dioxide

A custom-made particle formation system was used to produce free-flowing hollow solid lipid microparticles from fractionated palm oil and its blends with low-moisture butter. Details and operation of the particle formation system were reported previously (Yang and Ciftci, 2016). Briefly, the system contained a high-pressure syringe pump, a preheating section, a 100 mL high-pressure expansion vessel, a magnetic drive, temperature controllers, a depressurization valve, and a nozzle. Temperature of the expansion vessel was set to the lowest melting point of the solid lipid in pressurized CO_2 at 200 bar where the solid lipid is in its liquid state. Our previous studies showed that 200 bar and 50 µm nozzle diameter generated smaller ($d_{50\%}$ = 278 nm) hollow spherical particles (Yang and Ciftci, 2016); therefore, a 50 µm diameter nozzle was used. Temperature of the depressurization valve and nozzle was set to 130°C to prevent freezing due to the Joule-Thomson effect during atomization.

Firstly, fractionated palm oil or its blends with butter was fully melted at 130°C, and then 20 mL of the molten lipid sample was manually injected into the expansion vessel via the sampling port. Then, the expansion vessel was pressurized to 200 bar with CO_2 using the syringe pump. The pressurized CO_2 and lipid sample were mixed at 1000 rpm for 1 hour using the magnetic drive to form a CO_2-expanded lipid. The mixture was then allowed to stabilize for 10 min after the

magnetic drive was stopped. The pressure of the syringe pump was set to 10 bar above the pressure of the expansion vessel, the inlet valve was opened, and the depressurization valve was opened immediately, which allowed the CO_2-expanded lipid to be atomized through the nozzle. Finally, solid lipid particles were formed and collected in the sample collection vessel.

Fatty Acid Analysis

The fatty acid composition of the fractionated palm oil, low-moisture butter, palm oil-butter blends, as well as the obtained solid lipid particles was determined according to the AOAC Method 996.06 with some modifications (AOAC, 2001). Each sample (200 mg) was heated above its melting point, and 2 mL of triundecanoin ($C_{11:0}$) solution (5 mg mL^{-1} in chloroform) was added as an internal standard. Samples were dissolved in a 1:1 blend of chloroform and diethyl ether. A 14% BF_3/methanol reagent was added with toluene and the mixture was heated at 100°C in an oven for 45 min. After the mixture has been allowed to cool to room temperature, water (5 mL), hexane (1 mL), and sodium sulfate (1 g) were added. Layers of the mixture were allowed to separate, and the top layer containing fatty acid methyl esters was transferred for analysis. Fatty acid methyl esters were analyzed using a capillary GC equipped with a hydrogen flame-ionization detector. Separation was performed on a capillary column composed of fused silica (SP-2560; 100 m × 0.25 mm with 0.20 μm film thickness). Helium with a flow rate of 0.75 mL min^{-1} was used as the carrier gas. The injector and detector temperatures were set at 225 and 285°C, respectively. The initial column temperature was 100°C and held for 4 min before ramping at 3°C min^{-1} to a final temperature of 240°C, which was held for 15 min. Identification was done by comparing the retention times of the peaks with those of authentic fatty acid standards.

Particle Size and Size Distribution

A particle size analyzer based on laser diffraction (Mastersizer 3000, Malvern Instruments Ltd., Worcestershire, UK) was used to measure

the particle size and size distribution of the solid lipid particles. Approximately 30 mg of solid lipid particles were suspended in 25 mL distilled water with the addition of 0.4% (w/w) of polyoxyethylene sorbitan monooleate (Tween 80). Suspensions were then sonicated 30 min in an ultrasonic water bath (3510 R-MTH, Branson Ultrasonics Corporation, Danbury, CT, USA) before analysis. The range of 5–7% was used as the obscuration value. The refractive index (RI) of the lipid sample was set as 1.46. Distilled water (RI = 1.33) was used as the dispersant.

Particle Morphology

Scanning Electron Microscopy (SEM) Analysis

Particle morphology of the solid lipid particles was analyzed using a Field Emission-Scanning Electron Microscope (FE-SEM) (S4700, Hitachi High-Technologies Corporation, Tokyo, Japan). Double-sided carbon tape was used to mount a thin layer of the solid lipid particles. Then, a HiPace 80 (Pfeiffer Vacuum, Aßlar, Germany) sputter coated the lipid samples with chromium in an argon atmosphere. Particles were also freeze fractured prior to SEM imaging to present the hollow structure. The imaging was carried out at room temperature (21°C).

Atomic Force Microscopy (AFM) Analysis

The AFM analysis was performed to quantify the surface roughness of the palm oil-butter particles. The same samples used for SEM imaging were used for AFM analyses. AFM experiments were conducted using a Bruker Dimension Icon AFM with ScanAsyst automatic image optimization mode based on PeakForce Tapping (Santa Barbara, CA, USA). ScanAsyst-Air probe (k ~0.4 N m^{-1}, tip radius < 10 nm) (Bruker Corporation, Santa Barbara, CA, USA) was employed in all AFM measurements. The oscillation frequency was 2 kHz. All images were recorded in air and under atmospheric conditions (22°C, 25% RH). The scanning field was kept at 10 µm by 10 µm for all the particle samples. Two dimension (2D), three dimension (3D), and roughness data were acquired from the Nanoscope software package (Bruker Corporation,

Santa Barbara, CA, USA). The morphology of the surface sample was characterized by the arithmetic mean surface roughness (R_a):

$$R_a = \frac{1}{n} \sum_i^n \left| Z_i - Z_{ep} \right|$$

Z_{ep} is the height of the center plane, and Z_i is the *i*th height sample out of n total samples, as Z_i tends toward Z_{ep} surface roughness decreases. n is the number of samples within a given area.

Confocal Fluorescence Microscopy Analysis

The distribution of butter in hollow solid lipid particles of fractionated palm oil was investigated using a confocal fluorescence microscope (A1, Nikon Instruments Inc., Tokyo, Japan). Approximately 3–5 mg of solid lipid particles were firstly stained using 40 µL Nile Red solution (0.125%, w/v, in propane-1,2-diol) for 40 min before image collection. A fluorescence microscope (90i, Nikon Instruments Inc., Tokyo, Japan) was then used to record confocal images of z-series scanning by distance increments of 1.0 µm. Number of images was 14, 15, and 26 for particles obtained with only fractionated palm oil, 75% fractionated palm oil, and 50% fractionated palm oil, respectively. Excitation wavelengths of 561.6 and 640.9 nm and emission wavelengths of 570–620 and 663–738 nm were set to conduct the analysis for red and blue fluorophores, respectively. The imaging was carried out at room temperature (21°C).

Determination of the Particle Density

The bulk density (β) was determined in a 25 mL glass graduated cylinder as described by Quispe-Condori et al. (2011). Approximately 3 g of each sample (m) was weighed and poured through a funnel into the cylinder. The cylinder was then slightly tapped to collect the powders sticking to the cylinder wall off. The volume (V) was read directly and used to calculate the bulk density ($\beta = m/V$).

Determination of Melting Properties

The melting profile of the fractionated palm oil, low-moisture butter, blends, and the solid lipid particles were determined using a

differential scanning calorimeter (Pyris Diamond, Perkin Elmer, Waltham, MA, USA). A hermetically sealed aluminum pan was used to hold 5–7 mg of the samples, while an identical empty sealed pan served as the reference. The sample and reference pans were set in the calorimeter and allowed to equilibrate for 1 min at 25°C. Then, the samples were heated from 25 to 100°C at a heating rate of 5°C min^{-1}.

Determination of Polymorphism

Polymorphism of the solid lipid particles was determined using a PANalytical Empyrean Diffractometer unit (Empyrean, PANalytical, Westborough, MA, USA) at ambient temperature (21°C). The unit was operated with Cu Kα radiation with an intensity of 45 mA and a voltage of 40 kV. The incident beam path had a 20 mm mask and a divergence slit of 1/8°. Samples were stored at −18°C right after production and withdrawn in 2 days for polymorphism analysis. The solid lipid particles were placed in a stainless-steel holder with a 27 mm diameter and a pocket that is 2 mm deep. To improve the signal to noise ratio, the PIXcel detector had a diffracted beam monochromator. A spin rate of 22.5° s^{-1} was used during analysis. The continuous scan was run from 2 to 50° at 2θ min^{-1} with a step size of 0.026.

Statistical Analysis

Data are presented as mean _ standard deviation based on triplicate experiments and analyses. A single factor ANOVA was used to analyze differences within each Differential Scanning Calorimetry (DSC) data (onset melting temperature, peak melting temperature, offset melting temperature, and enthalpy value) among the samples (fractionated palm oil, low-moisture butter, their physical blends, and the obtained particles). SAS version 9.3 was the statistical software package used for all analyses (SAS Institute Inc., NC, USA). An alpha level of <0.05 was used to denote significance. Post hoc test was conducted by using Tukey's multiple comparison.

Results and Discussion

Melting Behavior in Pressurized CO_2

Understanding the melting behavior of the solid lipids in pressurized CO_2 is the key to select the lowest processing temperature to form particles via atomization of CO_2- expanded lipid. Previously, it was shown that the melting point of the fully hydrogenated canola oil decreased from 71 to 58°C in the pressurized CO_2 above 122 bar (Ciftci and Temelli, 2014), and that of fully hydrogenated soybean oil decreased from 68.5 to 57°C above 120 bar (Yang and Ciftci, 2016). Melting behavior of the fractionated palm oil and low-moisture butter in pressurized CO_2 is shown in Fig. 1. Melting point of the fractionated palm oil was 62.2°C under atmospheric conditions; however, it decreased to 47.3°C above 120 bar in pressurized CO_2. Similarly, the melting point of the low-moisture butter was 33.5°C under atmospheric conditions, and it decreased to 22.8°C above 55 bar. During mixing of the pressurized CO_2 and lipid, CO_2 dissolves in the liquid lipid and forms a CO_2-expanded lipid due to the dissolution of CO_2 in the lipid (Yang and Ciftci, 2016). Therefore, in the

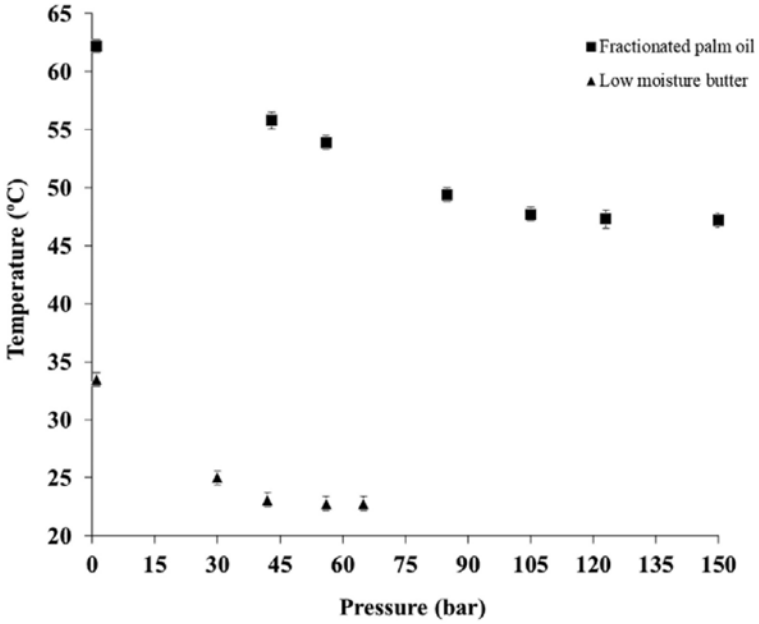

Fig. 1. Melting behavior of the fractionated palm oil and low-moisture butter in the pressurized CO_2.

high-pressure expansion vessel, two phases were formed; the upper SC-CO_2 phase consisting of mainly $SCCO_2$, and the bottom CO_2-expanded lipid phase. Only the bottom CO_2-expanded lipid phase is responsible for particle formation. The volumetric expansion of the lipids was reported previously to confirm the development of CO_2-expanded lipids (Ciftci and Temelli, 2014). Results confirmed that the lipid samples were in the liquid state during the expansion stage of the particle formation process. A CO_2- expanded lipid mixture is obtained due to dissolution of pressurized CO_2 in the lipid phase; therefore, the lipid must be in the liquid state to dissolve CO_2 in the lipid phase and to form an expanded lipid mixture. Melting point depression in pressurized CO_2 is important to optimize the particle formation conditions, and low processing temperature will also decrease the energy usage in the food industry.

Particle Morphology of the Hollow Solid Lipid Microparticles

SEM images of the solid lipid microparticles obtained with fractionated palm oil and its blends with low-moisture butter are shown in Fig. 2. All generated particles were spherical and free-flowing. The

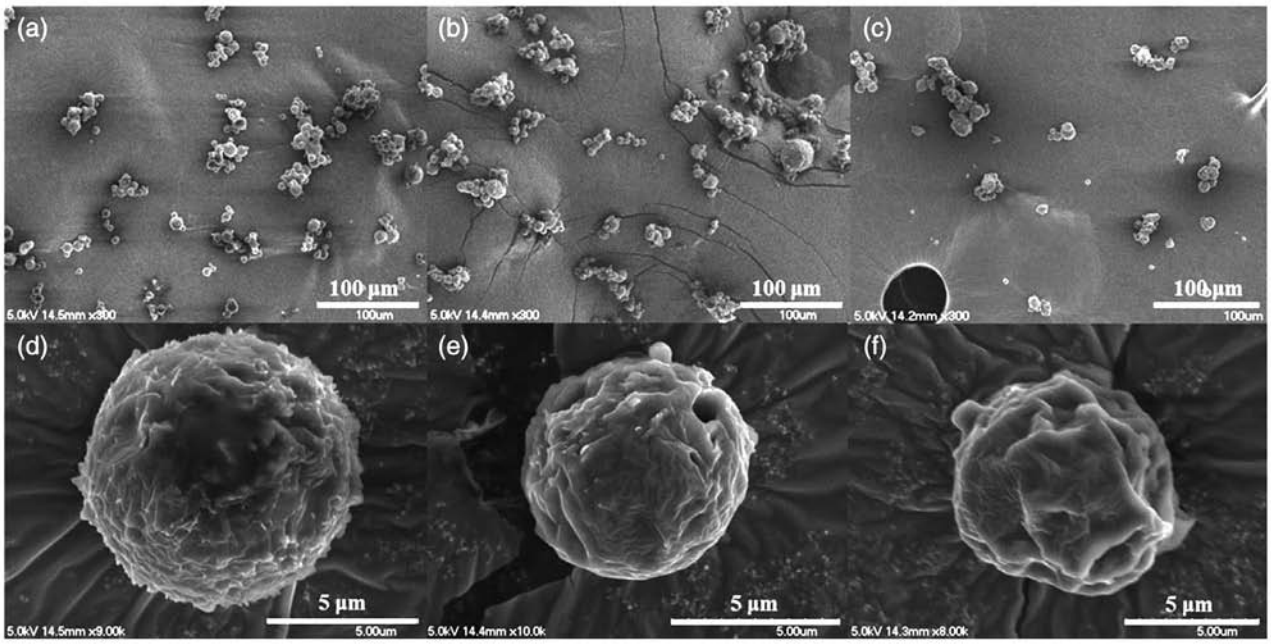

Fig. 2. SEM images of the solid lipid particles obtained at different lipid levels: (a, d) 100% fractionated palm oil; (b, e) 75% fractionated palm oil, 25% butter; and (c, f) 50% fractionated palm oil, 50% butter.

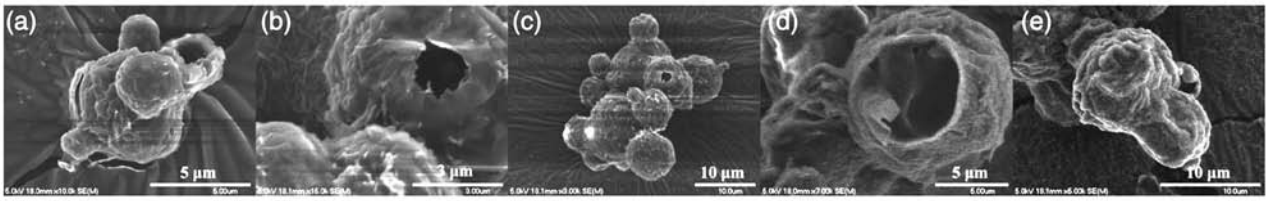

Fig. 3. SEM images of the freeze-fractured solid lipid particles: (a, b, c) 100% fractionated palm oil; (d) 75% fractionated palm oil, 25% butter; and (e) 50% fractionated palm oil, 50% butter.

hollow structure of the particles generated at all palm oil levels was observed from the SEM images of the freeze-fractured particles (Fig. 3). The particles had a wrinkled surface and increasing the butter content increased the wrinkled surface. Wrinkled surface formation was mainly due to melting point differences between butter and the fractionated palm oil. Butter has a lower melting temperature (38°C) than fractionated palm oil (67.7°C). When the CO_2-expanded lipid mixture is atomized at the nozzle upon depressurization, a liquid droplet of fractionated palm oil, butter, and SC-CO_2 was formed and then turned into a liquid lipid bubble due to CO_2 expansion at atmospheric pressure. In the meantime, temperature of the atomized particles decreased quickly due to the Joule-Thomson effect (Yang and Ciftci, 2016, 2017). During the sudden cooling, the liquid lipid droplet solidified immediately and formed solid lipid particles (Yang and Ciftci, 2016).

Fig. 4 presents the 3D surface topography of the palm oil–butter microparticles. The scale for 100% fractionated palm oil particles was 0–230 nm, whereas it was set at 0–1000 nm for 75% and 50%

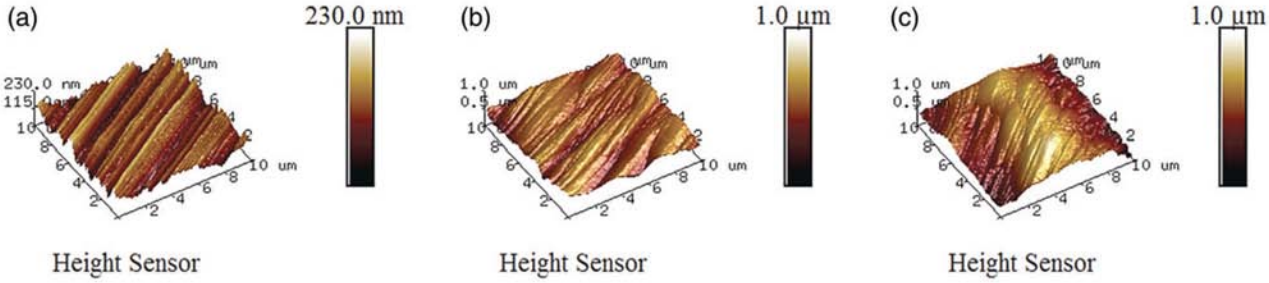

Fig. 4. 3D AFM images of the surface topography of the obtained palm-butter microparticles. (a) 100% fractionated palm oil; (b) 75% fractionated palm oil, 25% butter; and (c) 50% fractionated palm oil, 50% butter.

fractionated palm oil particles to include more specific details, and therefore rendering images a higher resolution. In agreement with the SEM images, the roughness and wrinkles on the particles' surface increased with increasing butter content in the lipid mixture. The mean surface roughness of the particles obtained with 100%, 75%, and 50% palm oil in the mixture was 21.9, 51.2, and 104 nm, respectively. When the higher melting fraction (palm oil) solidified, the lower melting fraction (butter) was still liquid and CO_2 was leaving the bubble toward outside, disturbing the smooth surface. Immediately after CO_2 released, the particle solidified and formed a wrinkled surface. The higher the solubility of CO_2 in the lipid phase, the higher wrinkled surface formation is expected because dissolution of the CO_2 in the lipid determines the melting point depression, which, in turn, determines the degree of the solidification rate. A faster solidification rate will form less-wrinkled surfaces compared to slow solidification. It was reported that the SC-CO_2 had higher solubility in the lower-melting fats than that of the higher counterparts, resulting in higher volumetric expansion (Ciftci and Temelli, 2014; Jenab and Temelli, 2012). Previously, it was found that the volumetric expansion of fully hydrogenated canola oil at 63°C and 150 bar was 12%, whereas it was 36% for cocoa butter (Calvignac et al., 2010; Ciftci and Temelli, 2014). When the butter concentration in the lipid mixture was increased, more CO_2 dissolved and the lipid droplet during atomization contained more CO_2. Therefore, more force was exerted on the inside of the liquid lipid bubble. During atomization, the quicker, more compact particle formation without butter did not allow wrinkles to form as prominently as it did in the slower solidifying butter-containing blends. With certain portions of the blend solidifying at different rates, the protruding portions of the sphere can be created.

In addition to SEM images, confocal fluorescence microscopy z-series scanning images that show the cross section of the spherical particles revealed that the microparticles were hollow (Fig. 5). Fig. 5 illustrated images taken at only a single slice during the z-series scanning of the particles, with a slice at the exact central location of the scanning in Fig. 5 (a, b, c) and a slice with a deeper scanning downward in Fig. 5 (d, e, f). The images in Fig. 5 (d, e, f) were auto-adjusted to improve the contrast to show the hollow structure of the particles. Some particles had one single large pore (hollow), and some particles had multiple relatively smaller pores (Fig. 5a, b, c) and when subjected

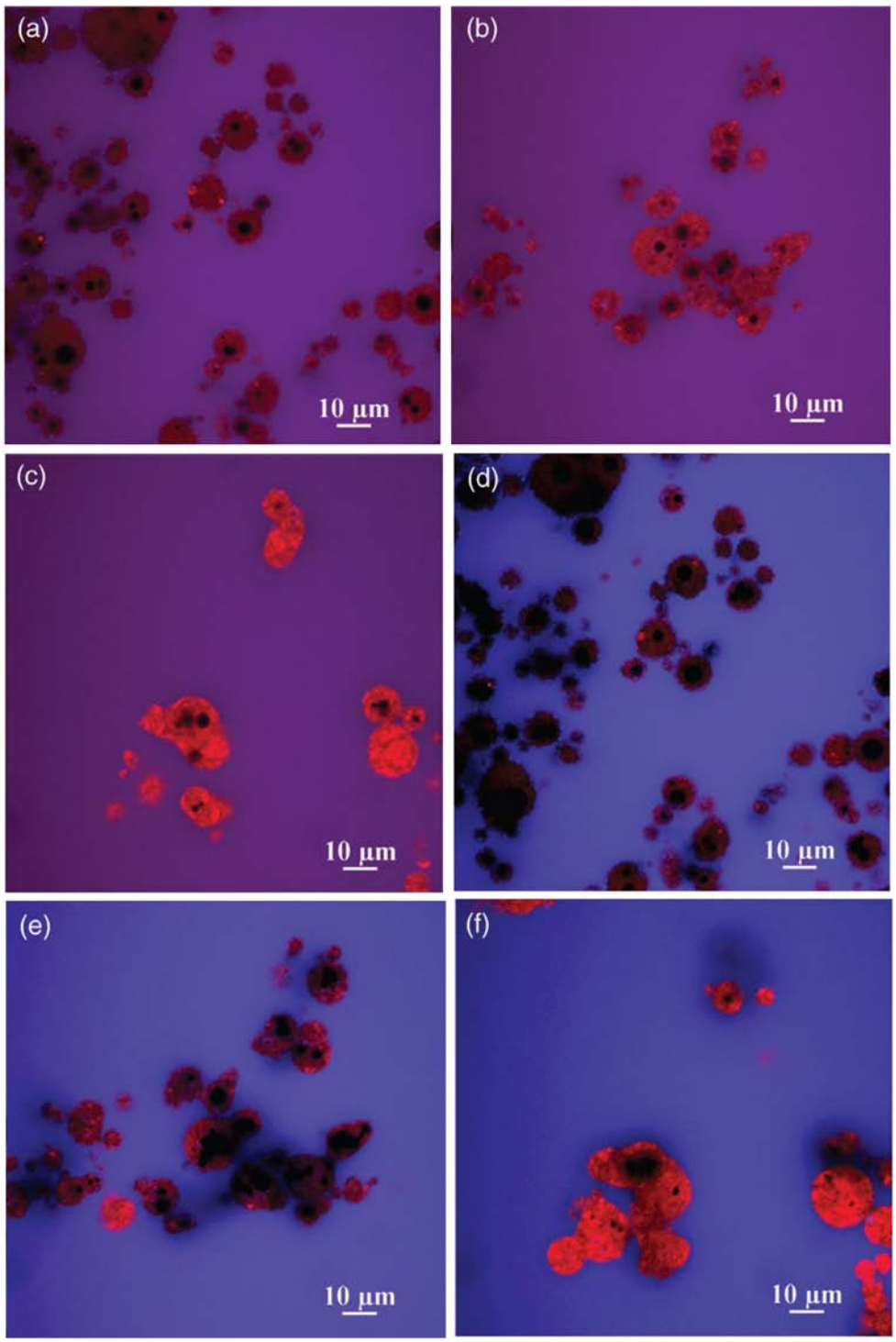

Fig. 5. Confocal fluorescence microscopy z-series scanning images of the solid lipid particles: (a, d) 100% fractionated palm oil; (b, e) 75% fractionated palm oil, 25% butter; and (c, f) 50% fractionated palm oil, 50% butter. The images are not z-stacked. (a, b, c) represent only a single slice of the central location of the scanning. Purple color represents the fluorescence from Nile Red staining solution as

to z-series scanning, these pores merged and created a big hollow sphere inside of the particle shell (Fig. 5d, e, f). Nile Red fluoresces differently depending on the degree of hydrophobicity of lipids, i.e., polar lipids such as phospholipids vs. neutral lipids such as triacylglycerols (Daemen et al., 2015; Diaz et al., 2008). The Nile Red psuedocolored blue/red ratio could be used to differentiate lipids (Diaz et al., 2008). The addition of butter to fractionated palm oil appeared as a brighter red color, because the fluorescent dye picked up both oils for staining. In addition, such a brighter color could also be due to slightly different emission intensities when bound to butter compared to fractionated palm oil. As expected, a higher butter content (50%) in the starting oil blend resulted in an increase in the red color intensity in the shell of the solid lipid particles, whereas there was no clear observation of the increased red color intensity in the hollow cavity.

Particle Density

Bulk density is a quality control parameter to assess the powdered particles. A dry product with high bulk density can be stored in small containers at the same amount to a product with low bulk density. The bulk density of the solid lipid particles obtained at different lipid levels is listed in Table 1. The bulk densities found in this study were

Table 1. Density of the fractionated palm oil and its blends with low-moisture butter, and of the solid lipid particles obtained at different lipid levels.

	Bulk density (kg m^{-3})[a]
Fractionated palm oil particles	169.2 ± 4.2
75% fractionated palm oil particles	143.2 ± 7.3
50% fractionated palm oil particles	141.7 ± 3.2
Fractionated palm oil	866.0 ± 63.2
75% fractionated palm oil blend	866.6 ± 58.8
50% fractionated palm oil blend	880.3 ± 70.9

a. Mean ± standard deviation, n = 3.

the background. (d, e, f) are auto-adjusted, and represent only a single slice of a deeper (after central) location of the scanning. Blue color represents the fluorescence from Nile Red staining solution as the background. Black color represents hollow structure in the particles; red color represents positive for Nile Red binding, indicating shell of the particles.

typical of encapsulated powders (Onwulata et al., 1996) with a few exceptions including microcapsules of a mixture of oil and acacia gum (Fuchs et al., 2006) and butter oil and modified corn starch (Onwulata et al., 1996). It was observed that the particles from the fractionated palm oil and the lipid matrix drastically reduced their bulk density (141– 169 kg m^{-3}) compared to their physical mixture counterparts (865–880 kg m^{-3}). The average bulk density of fractionated palm oil particles, 25% butter particles, and 50% butter particles was reduced by 80.5%, 83.5%, and 83.9%, respectively, when the solid physical blends were transformed into hollow solid lipid particles. The density reduction was caused by the hollow structure and small size of the particles as well as the packing spaces among the particles. Moreover, solid lipid particles produced from fractionated palm oil were denser (169 kg m^{-3}) than the particles with butter blends (141 kg m^{-3} for 50% butter). When used in food products, this reduction in density could provide key benefits. Less lipid materials can occupy more volume, which could allow for reduced material usage in food products with a fixed volume. The reduced material usage can also positively impact the nutrition of the food by reducing the number of fat grams and overall calories. The application of the particles obtained in this study could especially be impactful in lipids that have a high caloric density relative to other macronutrients.

Particle Size and Size Distribution

All particles exhibited a similar bimodal size distribution, which consisted of both nanoparticles and microparticles (Fig. 6). The mean

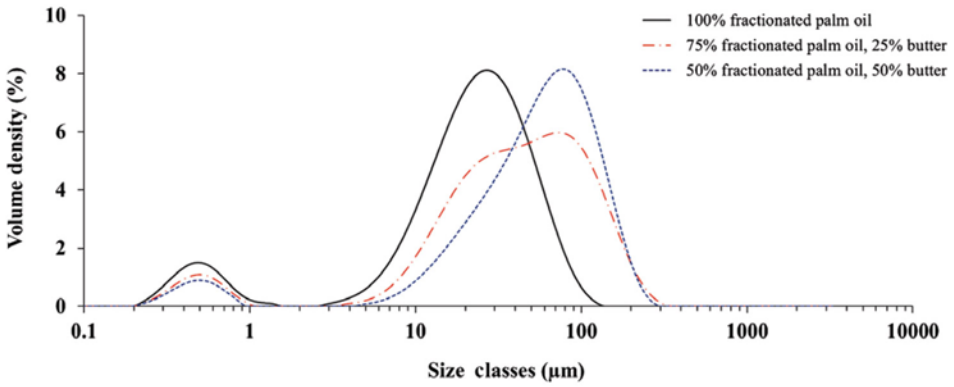

Fig. 6. Particle size distribution of the solid lipid particles.

particle size increased with butter content in the nonhydrogenated oil blends. The smallest particles were produced from the 100% fractionated palm oil (D [4, 3] = 27.1 μm). Ten percent ($d_{10\%}$) and 50% ($d_{50\%}$) of the particles were smaller than 4.5 and 23.0 μm, respectively, whereas they were 14.5 and 58.3 μm at 50% butter concentration, respectively (D [4,3] = 67.0 μm). A likely cause of the increasing particle size with higher levels of butter was the impact of the butter on the melting properties of the solid lipid particles, which in turn affected the solidification rate during particle formation (Yang and Ciftci, 2016). The addition of butter reduced the melting point of the particles, which solidified slowly during particle formation. The solidification rate was lower at increased butter concentrations due to lower melting point of the butter compared to the fractionated palm oil; the lipid bubble had more time to expand during atomization due to CO_2 release from the lipid bubble and formed larger hollow particles. It should be noted that the particle size results may be affected by the particle agglomeration in the samples with more butter content as well; therefore, it must be compared with the particle morphology analyses. When SEM images were compared, it was observed that the particle agglomeration occurred for all blends (Fig. 2). In addition, when confocal images were compared, the extent of particle agglomeration increased with butter concentration (Fig. 5). This was due to the blends of fractionated palm oil and butter made the lipid mixture viscous and the obtained particles sticky upon particle formation. However, particles generated at 50% butter content were still free-flowing at room temperature. Previously, Yang and Ciftci (2016) reported average particle sizes (D [4,3]) of 3.9–13.1 μm for the particles obtained from fully hydrogenated soybean oil with the same process. Rodrigues et al. (2004) formed theophylline/hydrogenated palm oil particles with a mean particle diameter of 3 μm using the PGSS technique; however, they did not report a hollow structure and the particle size was only of micron range.

Melting Properties

The melting properties of the fractionated palm oil and its blends with low-moisture butter are important to understand the characteristics of the obtained solid lipid particles including size distribution,

Table 2. DSC melting points and enthalpy of the lipid blends and the obtained solid lipid particles.

	Melting temperature (°C)			*Enthalpy ($J\ g^{-1}$)*
Sample	*Onset*	*Peak*	*Offset*	
Fractionated palm oil	62.0 ± 0.4a	67.7 ± 0.4a	69.0 ± 0.6a	106.7 ± 0.7a
75% fractionated palm oil	60.7 ± 0.3b	65.0 ± 0.5b	66.5 ± 0.5a	107.5 ± 0.6a
50% fractionated palm oil	56.3 ± 0.2c	60.0 ± 0.2cd	62.9 ± 0.3b	82.5 ± 0.6b
25% fractionated palm oil	54.1 ± 0.1d	58.0 ± 0.2e	60.6 ± 0.2c	34.9 ± 0.5e
Low-moisture butter	36.7 ± 0.1e	37.3 ± 0.1g	37.7 ± 0.1e	4.0 ± 0.2f
100% fractionated palm oil particles	57.3 ± 0.2c	61.0 ± 0.3c	62.7 ± 0.3b	105.3 ± 0.6a
75% fractionated palm oil particles	56.9 ± 0.1c	60.0 ± 0.2d	61.5 ± 0.3bc	48.7 ± 0.5c
50% fractionated palm oil particles	54.1 ± 0.1d	55.5 ± 0.2f	57.0 ± 0.2d	39.1 ± 0.4d

Results were expressed as mean ± standard deviation, $n = 3$. Means with different letters within the same column are significantly different ($P < 0.05$) according to Tukey's multiple range test.

particle morphology, and polymorphism. Table 2 present the DSC melting points of the original nonhydrogenated oils and their blends, the generated solid lipid particles from fractionated palm oil and its selected mixtures with low-moisture butter, respectively, and Fig. 7 shows the DSC melting curves of the solid lipid particles. The major melting point of the fractionated palm oil was higher than that of the blends with low-moisture butter that possessed the lowest. Moreover, with increasing levels of butter to fractionated palm oil from 25% to 75%, the melting peak temperature of the physical blends significantly decreased from 65 to 58°C ($P < 0.05$) due to the presence of more

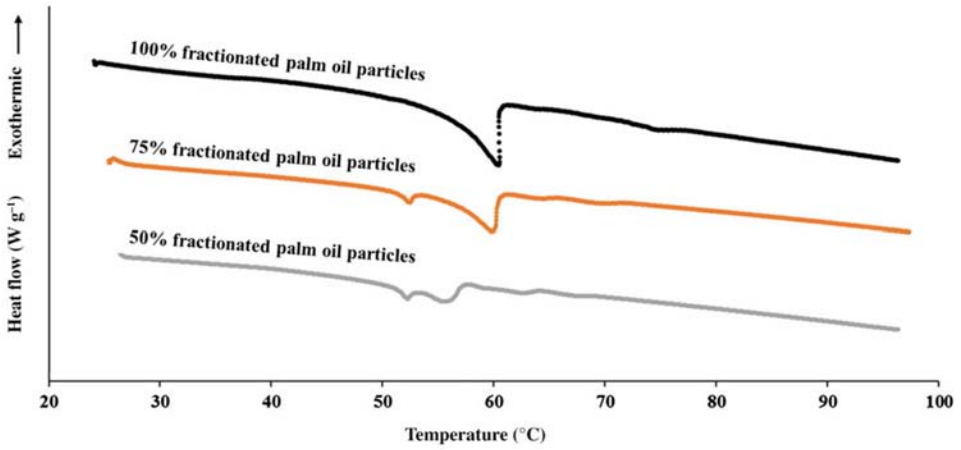

Fig. 7. DSC melting curves of the solid lipid particles obtained from the blends of fractionated palm oil and low-moisture butter.

unsaturated fatty acids making the mixture in a less-ordered packing with less solid fat content (Table 3). After the particle formation process, even though the fatty acid compositions were similar, solid lipid particles exhibited a different melting profile compared to their physical bulk oil. The original fractionated palm oil and its blends with butter, which was at 25% and 50% concentration, had a major melting peak temperature around 60–67.7°C, whereas the solid lipid particles exhibited a stepwise melting pattern and shifted the melting temperature to a relatively lower temperature. The original fractionated palm oil melted between 62 and 69°C with a major endothermic peak of 67.7°C; however, the single endothermic melting peak was significantly reduced to 61°C for its solid lipid particles counterpart ($P < 0.05$). A similar significant decrease in the major melting peak temperature was also observed for lipid particles obtained from 25% and 50% butter concentrations ($P < 0.05$). This major melting peak temperature decrease was attributed to the smaller particle size, hollow structure with a thin shell, and polymorphic forms (discussed below in Polymorphism Section). In solid lipid particles from nonhydrogenated oil blends, two melting peaks were depicted, with 53°C

Table 3. Composition of the major fatty acids (%) of low-moisture butter, fractionated palm oil (FPO), their physical blends[a], and the obtained particles[b]

Composition	*Butter*	*FPO*	*FPO-P*	*75% FPO*	*75% FPO-P*	*50% FPO*	*50% FPO-P*
Caproic acid (6:0)	2.4	0.0	0.0	0.5	0.5	1.1	1.0
Caprylic acid (8:0)	1.3	0.0	0.0	0.3	0.3	0.6	0.6
Capric acid (10:0)	3.1	0.0	0.0	0.7	0.7	1.5	1.4
Lauric acid (12:0)	3.5	0.2	0.2	1.0	1.0	1.8	1.7
Myristic acid (14:0)	11.3	1.3	1.3	3.6	3.5	6.2	5.7
Myristoleic acid (14:1)	1.4	0.0	0.0	0.3	0.2	0.7	0.6
Palmitic acid (16:0)	31.1	77.8	78.7	68.2	68.3	55.7	57.9
Palmitoleic acid (16:1)	2.1	0.0	0.0	0.5	0.5	1.0	0.9
Stearic acid (18:0)	10.8	5.0	5.0	6.2	6.4	7.8	7.5
Oleic acid (18:1, n-9)	21.4	12.3	11.6	13.7	12.7	16.4	14.1
Vaccenic acid (18:1, trans)	2.1	0.0	0.0	0.0	0.0	1.2	0.0
Linoleic acid (18:2, n-6)	3.2	2.3	2.1	2.4	2.3	2.7	2.3
SFA	54.6	75.9	78.5	71.3	73.8	65.7	70.3
MUFA	22.0	11.1	10.8	13.0	12.8	16.4	15.3
PUFA	3.4	2.1	2.0	2.2	2.1	2.7	2.2

a. 75% FPO: 75% fractionated palm oil, 25% butter; 50% FPO: 50% fractionated palm oil, 50% butter.

b. FPO-P: 100% fractionated palm oil; 75% FPO-P: 75% fractionated palm oil, 25% butter; 50% FPO-P: 50% fractionated palm oil, 50% butter; SFA: Saturated fatty acids; MUFA: Monounsaturated fatty acids; and PUFA: Polyunsaturated fatty acids.

being the lower peak for both oils and 55.5 or 60°C being the second peak, depending on the lipid composition. The presence of the lowest melting peak of 53°C was attributed to the nanosize portion of the lipid particles (Yang and Ciftci, 2016). Particle size plays a crucial role in melting temperature of colloidal substances; melting temperature decreases with decreasing particle size (Defay et al., 1966). Interestingly, no melting peak of 53°C shown in lipid particles of fractionated palm oil. This was due to the agglomeration of the nanoparticles. The presence of nanoparticles in the solid lipid particles was evidenced in the particle size analysis (Fig. 6). Moreover, the addition of a less-saturated fat, i.e., low-moisture butter, to fractionated palm oil resulted in formation of a relatively less-ordered crystals of the lipid particles and led to a significant reduction in the melting point ($P < 0.05$). This phenomenon became more pronounced when 50% butter mixed with the fractionated palm oil, the major melting peak temperature decreased to 55.5°C compared to 61 and 60°C at 0% and 25% butter concentrations, respectively.

Polymorphism

Polymorphism is an important parameter that affects the melting properties of the solid lipid particles. Fats can crystallize in three main polymorphic forms, namely α, β, and β′. The polymorphic form of α is the least stable whereas β is the most stable, and β′ is metastable (Rousseau et al., 1998). Polymorphic form of α melts at a lower temperature compared to β′ and β forms, which is due to less-organized packing of triacylglycerol molecules within the lattice resulted from its less-stable crystal structure (Lawler and Dimick, 2008; Yang and Ciftci, 2016). Fig. 8 reveals that the addition of low-moisture butter to fractionated palm oil affected the polymorphism of the solid lipid particles. The polymorphic forms are characterized by short spacings (d) obtained from X-ray diffraction (XRD) patterns, which were defined as the distance due to lateral packing of the fatty acid chains on the triacyglycerol molecules (ten Grotenhuis et al., 1999). The short spacings of 0.46, 0.37, and 0.38 nm indicated that fractionated palm oil being β and β′ crystalline structures, whereas butter addition resulted in primarily α ($d = 0.41$ nm) form. After the particle formation process, solid lipid particles of fractionated palm oil still exhibited β and β′ forms but with

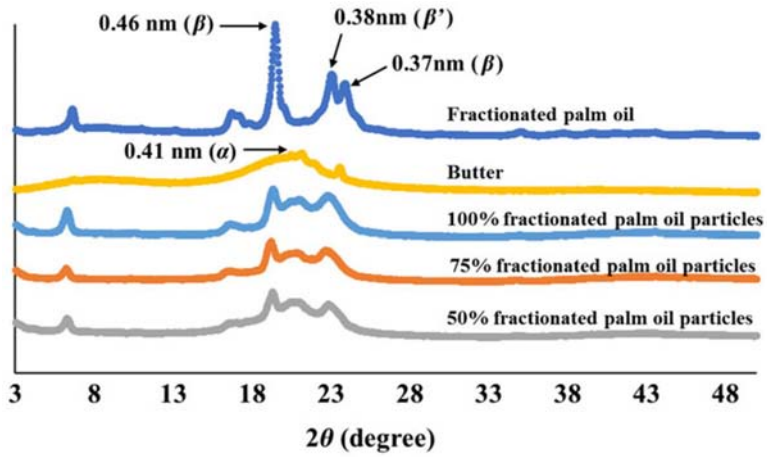

Fig. 8. XRD patterns of the solid lipid particles obtained from the blends of fractionated palm oil and low-moisture butter.

reduced intensity. Both observations indicated that the solid lipid particles were less ordered in the crystalline structure than the original bulk oil, which is supported by the DSC melting curves (Fig. 7). In solid lipid particles generated from blends of fractionated palm oil and butter, the distribution of α, β, and β′ polymorphic forms appeared to be quite similar to the particles obtained from fractionated palm oil but with a slight further decrease of β form intensity. This was due to the introduction of butter with relatively lower melting temperature to the mixture, therefore contributing to the less stability of the crystalline structure in the solid lipid particles. The solid lipid particles obtained in this study are hollow and dense-packed, which can be the advantages to develop low-calorie, easy-to-use butter ingredients/foods without the need for refrigeration.

Conclusions

This study demonstrates that nonchemically modified lipids can be used to form hollow microparticles, and possibly nanoparticles, via rapid depressurization of a CO_2- expanded lipid. Lower-melting fats with desirable characteristics such as butter for their flavor can be blended with higher-melting lipids to be incorporated into the particles. The reported process reduced the density of the particles five-folds compared to that of the raw solid fats, decreased the melting

point, and increased the surface area due to microparticle formation. There are a number of potential unique, beneficial applications of the obtained hollow solid lipid particles. Free-flowing particles enable easier handling of solid fat materials. These particles could also allow solid fats to be incorporated uniformly into foods. Compared to many common forms of solid fat, the particles created in this study have a much higher ratio of surface area to mass due to their hollow nature and small size. When incorporated into foods, the increased surface area could allow for additional oil coating on the palate so less material could be used while still achieving the same oil mouthfeel, which could be especially valuable in reduced fat and calorie foods. The increased ratio of surface area to mass contributes to quicker melting when the particles are in contact with a heat source as well. This attribute could potentially allow for consumed fats to melt quicker on the palate, which could help to reduce the undesirable fatty mouth coating that occurs when lipids with high melting points are consumed and stay in their solid state. These properties could also be applied as unique functional benefits in certain types of foods. For example, the particles could be used in a drink mix powder that is stirred into a warm liquid. The high ratio of surface area to mass allows the particles to have additional contact with the liquid causing quicker melting and mix in.

Acknowledgments — This project is based on research that was supported by the Hatch Multistate Research capacity funding program (Accession Number 1011129) from the USDA National Institute of Food and Agriculture, and the Office of Research and Economic Development (ORED) at the University Nebraska–Lincoln. Authors thank ConAgra Brands for GC analysis and providing solid lipid samples.

The authors declare that they have no conflict of interest.

References

AOAC International (2001) AOAC Method 996.06. *Journal of AOAC International*, 41.1.28A.

Bertucco, A., Caliceti, P., & Elvassore, N. (2007) Process for the production of nano-particles. *Patent No. WO2007028421 A1*. International Search Report, Rijswijk, Netherlands.

Calvignac, B., Rodier, E., Letourneau, J., dos Santos, P. M. A., & Fages, J. (2010) Cocoa butter saturated with supercritical carbon dioxide: Measurements

and modelling of solubility, volumetric expansion, density and viscosity. *International Journal of Chemical Reactor Engineering*, 8:A73.

Ciftci, O. N., & Temelli, F. (2014) Melting point depression of solid lipids in pressurized carbon dioxide. *Journal of Supercritical Fluids*, 92:208–214.

Daemen, S., van Zandvoort, M. A. M. J., Parekh, S. H., & Hesselink, M. K. C. (2015) Microscopy tools for the investigation of intracellular lipid storage and dynamics. *Molecular Metabolism*, 5:153–163.

Defay, R., Prigogine, I., Bellemans, A., & Everett, D. H. (1966) *Surface tension and adsorption*. New York, NY: Wiley.

Diaz, G., Melis, M., Batetta, B., Angius, F., & Falchi, A. M. (2008) Hydrophobic characterization of intracellular lipids in situ by Nile red red/yellow emission ratio. *Micron*, 39:819–824.

Dietz, W. H., & Scanlon, K. S. (2012) Eliminating the use of partially hydrogenated oil in food production and preparation. *Journal of the American Medical Association*, 308:143–144.

Downs, S. M., Gupta, V., Ghosh-Jerath, S., Lock, K., Thow, A. M., & Singh, A. (2013) Reformulating partially hydrogenated vegetable oils to maximise health gains in India: Is it feasible and will it meet consumer demand? *BMC Public Health*, 13:1139.

Fahim, T. K., Zaidul, I. S. M., Abu Bakar, M. R., Salim, U. M., Awang, M. B., Sahena, F., … Sohrab, M. H. (2014) Particle formation and micronization using non-conventional techniques— Review. *Chemical Engineering and Processing: Process Intensification*, 86:47–52.

Fuchs, M., Turchiuli, C., Bohin, M., Cuvelier, M. E., Ordonnaud, C., Peyrat-Maillard, M. N., & Dumoulin, E. (2006) Encapsulation of oil in powder using spray drying and fluidized bed agglomeration. *Journal of Food Engineering*, 75:27–35.

García-González, C. A., Argemí, A., Sampaio de Sousa, A. R., Duarte, C. M. M., Saurina, J., & Domingo, C. (2010) Encapsulation efficiency of solid lipid hybrid particles prepared using the PGSS technique and loaded with different polarity active agents. *Journal of Supercritical Fluids*, 54:342–347.

Jenab, E., & Temelli, F. (2012) Density and volumetric expansion of carbon dioxide-expanded canola oil and its blend with fully hydrogenated canola oil. *Journal of Supercritical Fluids*, 70:57–65.

Lawler, P. J., & Dimick, P. S. (2008) Crystallization and polymorphism of fats. In C. C. Akoh & D. B. Min (Eds.), *Food lipids: Chemistry, nutrition and biotechnology* (p. 253). Boca Raton, FL: CRC Press.

Lubary, M., de Loos, T. W., ter Horst, J. H., & Hofland, G. W. (2011) Production of microparticles from milk fat products using the supercritical melt Micronization (ScMM) process. *Journal of Supercritical Fluids*, 55:1079–1088.

Mandžuka, Z., & Knez, Ž. (2008) Influence of temperature and pressure during PGSS micronization and storage time on degree of crystallinity and crystal forms of monostearate and tristearate. *Journal of Supercritical Fluids*, 45:102–111.

Onwulata, C. I., Konstance, R. P., & Holsinger, V. H. (1996) Flow properties of encapsulated milk fat powders as affected by flow agent. *Journal of Food Science*, 61:1211–1215.

Quispe-Condori, S., Saldaña, M. D. A., & Temelli, F. (2011) Microencapsulation of flax oil with zein using spray and freeze drying. *LWT - Food Science and Technology*, 44:1880–1887.

Rodrigues, M., Peiriço, N., Matos, H., Gomes de Azevedo, E., Lobato, M. R., & Almeida, A. J. (2004) Microcomposites theophylline/hydrogenated palm oil from a PGSS process for controlled drug delivery systems. *Journal of Supercritical Fluids*, 29: 175–184.

Rousseau, D., Marangoni, A. G., & Jeffrey, K. R. (1998) The influence of chemical interesterification on the physicochemical properties of complex fat systems: 2. Morphology and polymorphism. *Journal of the American Oil Chemists' Society*, 75:1833–1839.

Sampaio de Sousa, A. R., Simplício, A. L., de Sousa, H. C., & Duarte, C. M. M. (2007) Preparation of glyceryl monostearate-based particles by PGSS - application to caffeine. *Journal of Supercritical Fluids*, 43:120–125.

ten Grotenhuis, E., van Aken, G. A., van Malssen, K. F., & Schenk, H. (1999) Polymorphism of milk fat studied by differential scanning calorimetry and real-time X-ray powder diffraction. *Journal of the American Oil Chemists' Society*, 76:1031–1039.

Ubeyitogullari, A., & Ciftci, O. N. (2016) Phytosterol nanoparticles with reduced crystallinity generated using nanoporous starch aerogels. *RSC Advances*, 6:108319–108327.

Watson, E. (2018) In conversation with Cargill: Which fats do consumers think are healthiest (and are they on the same page as nutrition scientists)?. Online https://www.foodnavigator-usa.com/Article/2018/05/18/In-conversation-with-Cargill-Which-fats-do-consumers-think-are-healthiest#

Yang, J., & Ciftci, O. N. (2016) Formation of hollow solid lipid micro- and nanoparticles using supercritical carbon dioxide. *Food and Bioproducts Processing*, 98:151–160.

Yang, J., & Ciftci, O. N. (2017) Encapsulation of fish oil into hollow solid lipid micro- and nanoparticles using carbon dioxide. *Food Chemistry*, 231:105–113.